

## **FRACTAL SPACE BASED DIMENSIONLESS ANALYSIS OF THE SURFACE SETTLEMENT INDUCED BY THE SHIELD TUNNELING**

**Yuan Mei<sup>1</sup>, Xinyu Tian<sup>1</sup>, Xuejuan Li<sup>2</sup>, Khaled Gepreel<sup>3</sup>**

<sup>1</sup>School of Civil Engineering, Xi'an University of Architecture and Technology,  
Xi'an, China

<sup>2</sup>School of Science, Xi'an University of Architecture and Technology, Xi'an, China

<sup>3</sup>Department of Mathematics, College of Science, Taif University, Taif, Saudi Arabia

**Abstract.** *The surface settlement during the tunneling process is becoming increasingly difficult to forecast as its surroundings become more and more erratic, and the maximal surface settlement raises risks posed suddenly by various uncertain factors. This paper proposes a novel approach to prediction of the surface settlement and analyzes the stability of tunnel construction. The dimensionless analysis and Buckingham's  $\pi$ -theorem are adopted for this purpose, and some useful dimensionless quantities are found, which can be used to determine the surface settlement's main properties. In this manner, the paper offers new ways of predicting surface settlement in various cases, and it sheds a new light on the tunnel's design and safety monitoring.*

**Key words:** *Surface settlement, Shield tunneling, Dimensionless analysis, Buckingham's  $\pi$ -theorem, Fractal space*

### 1. INTRODUCTION

Due to the rocketing urbanization in China, and generally in the world, the shield tunneling becomes the main tool for the subway construction. However, various accidents were reported, among which the surface settlement is the most serious problem, which might lead to an abrupt disaster of buildings damage and injuries. The shield tunneling induce accidents with fatal outcome to a similar amount as traffic accidents. So far there is neither a universal approach to reliable preventing the disaster, nor an effective method to predict the maximal surface settlement at the initial stage. The surface settlement is an extremely complex process with many influencing factors, making it impossible to estimate and control

---

Received: August 26, 2023 / Accepted November 30, 2023

**Corresponding author:** Xuejuan Li

School of Science, Xi'an University of Architecture and Technology, Xi'an, China

E-mail: lxj\_zk@163.com

the settlement process. The influencing factors include mainly the geological structure, the shield tunneling machine's parameters and the tunnel geometrical property.

Though there are some empirical methods for prediction of surface settlement, the theoretical analysis was rare and rather preliminary [1-4]. A modified empirical Peck formula was used to predict the surface settlement in water-rich sandy cobble strata [5]. Lu et al. [6] suggested a Gaussian function model based on a large number observation data of surface settlements, which can describe the geometrical shape of surface settlement. Based on the Mair's theory, Yang et al. [7] proposed a computational method for long-term settlement of the soil at surface and subsurface, while Macklin [8] used the load factor parameter to predict the volume loss. All empirical methods have obvious limitations that they need all tunneling conditions, which are difficult to be obtained. It is extremely difficult to establish a theoretical model, though many scientists have been trying to develop a universal theory [9-11], without a definite success. An alternative approach is provided by versatile numerical methods [12-14], but the unknown boundary conditions and unknown ground properties prevented successful numerical analyses in practical applications. The big data theory and the machine learning became a hot topic because of their versatile applications to majority of complex problems [15-19]. Though some success has been achieved in forecasting the surface settlement [20-22], the machine learning method is not a method of choice for the tunneling process, as the missing data makes the real-time prediction impossible.

Hence, the research roads diverged in the tunneling process, and currently there is no generally accepted approach for prediction of the surface settlement. Therefore, this paper sets the objective to propose a new approach – dimensionless analysis. Though the method is generally known in engineering [23], it has never been used for this specific purpose.

Using the dimensionless analysis, Estrada-Diaz et al. [24] found a very useful mathematical model for predicting the dynamical properties of the electrospinning process, and the complex dynamic spinning process of critical importance for nanotechnology [25-27] became suddenly accessible to engineers. He et al. [28] obtained an important bond stress-slip relationship for 3-D printed concretes. Kong and He [29] found a totally new friction law for porous surfaces, and Coulomb's empirical law was abandoned completely in the textile engineering [30]. Prakash et al. [31] found the main factors affecting the rotor-bearing system's dynamical property. Ma [32] elucidated successfully the transient thermal properties. Silva et al. [33] established a relationship among linguistic variables. Recently, He and Liu [34] pointed out a possible link between the fractal dimensions and the exponents involved in the dimensionless analysis, pushing the dimensionless analysis to the research frontiers in various fields, e.g., mathematics, physics, mechanical engineering and material science.

In this paper, we apply the dimensionless analysis to the analysis of a seemingly complex problem of the surface settlement during the tunneling process, taking into account the geological structure, the shield tunneling machine's property and the tunnel's geometrical property.

## 2. DIMENSIONAL ANALYSIS METHOD

Engineers have been facing intractable settlement behaviors [35]. Wang et al. [36] established a mechanical model and solved it analytically, and in order to obtain the analytical solution, some unnecessary assumptions had to be made, thus rendering the model to be mainly of mathematical interest. Pichler, et al. [37] gave a thermo-chemo-mechanical assessment to improve the tunneling process. Tong et al. [38] suggested an improved model for a shallow tunnel in a semi-infinite plane. Though the above models can account for out some properties of the settlement and for some special cases, there is no universal one applicable to a general tunneling process.

The shield tunneling process is an interdisciplinary subject among civil engineering, mechanical engineering and mechanics. The engineering failure analysis [39] and the typical structural elements of shield tunnels [40] are widely used in the process. In this paper, the dimensionless analysis, which is widely used in mechanical engineering and fluid mechanics, is adopted to analyze the main factors affecting the tunneling-induced settlement.

The dimensionless analysis is an approach widely used in science and engineering for complex problems. The most famous achievement is the Reynolds number [41] in fluid mechanics, which has been widely used to identify the turbulent flow. Other famous dimensionless quantities include Nusselt number and Prandtl number for the boundary layer theory [42], Eckart number for heat dissipation [43], Hartmann number for electro-magneto-nanofluids [44, 45].

The dimensionless analysis is also widely applied to deal with intractable problems arising in mechanical engineering, e.g., the leakage performance of a seal [46], plastic deformation [47], and non-inertial stopping performance [48]. It is used to study the relation among physical quantities based on their units and dimensions, offering a totally new window for analyzing a complex problem with a simple mathematical treatment. In the engineering problems, it is necessary to keep the same units, and it helps understand physical laws and relationship among various factors [49]. The fundamental dimensions are mass ( $M$ ), length ( $L$ ), and time ( $T$ ).

## 3. INFLUENCING FACTORS ANALYSIS

For the surface settlement during the tunneling process, we have to consider the geological feature, the shield tunneling machine's parameters and the tunnel's geometrical shape. In this section, we will analyze the main influencing factors from the above three aspects.

### 3.1. Geological parameters

The surface settlement depends heavily on the soil types. Fig. 1 shows some fundamental soils. During the tunneling process, the soil's dynamical parameters are needed to study the surface's settlement. In this paper, we choose 11 physical quantities of soil dynamics, e.g., dynamic viscosity, particle diameter, pore water pressure, permeability, density, elastic modulus, effective stress, for the dimensional analysis in tunneling processes. Their symbols, units, and dimensions are shown in Table 1.

**Table 1** Physical quantities of soil dynamics in the dimensional analysis

Physical quantity	Symbol	Units	Dimensions
Dynamic viscosity	$\eta$	Pa.s	$ML^{-1}T^{-1}$
Particle diameter	$D$	mm	$L$
Pore water pressure	$p_p$	MPa	$ML^{-1}T^{-2}$
Permeability	$k$	$m^2$	$L^2$
Face pressure	$p_f$	MPa	$ML^{-1}T^{-2}$
Density	$\rho$	$Kg/m^3$	$ML^{-3}$
Elastic modulus	$E_e$	MPa	$ML^{-1}T^{-2}$
Stress	$\sigma$	MPa	$ML^{-1}T^{-2}$
The soil volume	$V_g$	$m^3$	$L^3$
Pore volume	$V_p$	$m^3$	$L^3$
Gravity acceleration	$g$	$m/s^2$	$LT^{-2}$

**Fig. 1** Geological structure

### 3.2. Shield tunneling machine parameters

Various shield modes can be chosen according to the soil's property. Taking the earth pressure balance shield as an example, we can identify legitimately the important parameters of the shield tunneling machine as given in Table 2.

**Table 2** Physical quantities of the shield tunneling machine in the dimensional analysis

Physical quantity	Symbol	Units	Dimensions
Jack thrust	$F$	T(9.8KN)	$MLT^{-2}$
Penetration rate	$v$	mm/min	$LT^{-1}$
Grout filling pressure	$p_j$	Mpa	$ML^{-1}T^{-2}$
Grouting quantity	$Q_j$	$m^3/\text{ring}$	$L^3$
Soil bin pressure	$p_b$	Mpa	$ML^{-1}T^{-2}$
Cutter torque	$N_c$	KN.m	$ML^2T^{-2}$
Cutter rotate speed	$w_c$	rpm	$T^{-1}$
Cutter diameter	$D_c$	m	$L$

### 3.3. Tunnel geometrical parameters

Generally, the tunnel geometrical parameters are unchanged. In this research, only the cover depth and the tunnel's radius are considered as influence factors. Fig. 2 shows the

diagram of the tunnel geometric characteristics and Table 3 gives the information of physical quantities for the dimensional analysis.

**Table 3** Physical quantities of the tunnel’s geometrical shape in the dimensional analysis

Physical quantity	Symbol	Units	Dimensions
Cover depth	$H$	m	$L$
The tunnel radius	$R$	m	$L$

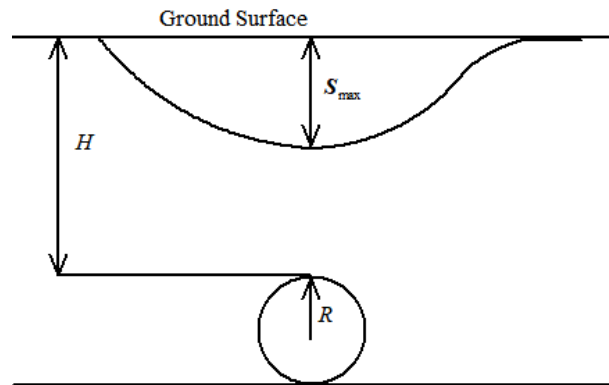


**Fig. 2** The diagram of tunnel geometric characteristics

#### 4. DIMENSIONAL ANALYSIS MODEL

In order to investigate the relationship among the variables involved in the soil dynamics (11 physical quantities), the shield tunneling machine (8 physical quantities) and the tunnel’s geometrical shape (2 physical quantities) by Buckingham’s  $\pi$ -theorem [49], all parameters in the Tables 1, 2 and 3 are chosen as the independent physical quantities. We can assume that

$$\varphi(F, v, p_j, Q_j, p_b, N_c, w_c, D_c, \eta, D, p_p, k, p_f, \rho, E_e, \sigma, V_g, V_p, g, H, R, S_{max}) = 0 \quad (1)$$

According to Eq. (1) and Buckingham’s  $\pi$ -theorem, the calculation formula of the  $\pi$  term is

$$F^{a_1} \cdot v^{a_2} \cdot p_j^{a_3} \cdot Q_j^{a_4} \cdot p_b^{a_5} \cdot N_c^{a_6} \cdot w_c^{a_7} \cdot D_c^{a_8} \cdot \eta^{b_1} \cdot D^{b_2} \cdot p_p^{b_3} \cdot k^{b_4} \cdot p_f^{b_5} \cdot \rho^{b_6} \cdot E_e^{b_7} \cdot \sigma^{b_8} \cdot V_g^{b_9} \cdot V_p^{b_{10}} \cdot g^{b_{11}} \cdot H^{c_1} \cdot R^{c_2} \cdot S_{max}^a = \pi \quad (2)$$

where  $\pi$  is the dimensionless quantity;  $a_1 \sim a_8$ ,  $b_1 \sim b_{11}$ ,  $c_1$ ,  $c_2$  and  $a$  are the exponents corresponding to all physical parameters. Substituting all dimensions into Eq. (2), we re-write Eq. (2) in the form

$$\begin{aligned}
 & [MLT^{-2}]^{a_1} [LT^{-1}]^{a_2} [ML^{-1}T^{-2}]^{a_3} [L^3]^{a_4} [ML^{-1}T^{-2}]^{a_5} [ML^2T^{-2}]^{a_6} [T^{-1}]^{a_7} [L]^{a_8} \cdot \\
 & [ML^{-1}T^{-1}]^{b_1} [L]^{b_2} [ML^{-1}T^{-2}]^{b_3} [L^2]^{b_4} [ML^{-1}T^{-2}]^{b_5} [ML^{-3}]^{b_6} \cdot \\
 & [ML^{-1}T^{-2}]^{b_7} [ML^{-1}T^{-2}]^{b_8} [L^3]^{b_9} [L^3]^{b_{10}} [LT^{-2}]^{b_{11}} \cdot [L]^{c_1} [L]^{c_2} \cdot [L]^a = [L]^0 [M]^0 [T]^0
 \end{aligned} \tag{3}$$

According to the principle of dimension homogeneity, we have  
 [L]:

$$a_1 + a_2 - a_3 + 3a_4 - a_5 + 2a_6 + a_8 - b_1 + b_2 - b_3 + 2b_4 - b_5 - 3b_6 - b_7 - b_8 + 3b_9 + 3b_{10} + b_{11} + c_1 + c_2 + a = 0 \tag{4}$$

[M]:

$$a_1 + a_3 + a_5 + a_6 + b_1 + b_3 + b_5 + b_6 + b_7 + b_8 = 0 \tag{5}$$

[T]:

$$-2a_1 - a_2 - 2a_3 - 2a_5 - 2a_6 - a_7 - b_1 - 2b_3 - 2b_5 - 2b_7 - 2b_8 - 2b_{11} = 0 \tag{6}$$

For the convenience of analysis, we rewrite Eqs. (4-6) as follows

$$\mathbf{A}y = 0 \tag{7}$$

where  $y=(a_1, a_2, a_3, a_4, a_5, a_6, a_7, a_8, b_1, b_2, b_3, b_4, b_5, b_6, b_7, b_8, b_9, b_{10}, b_{11}, c_1, c_2, a)^T$  is the column vector of the exponents and the dimensional matrix  $\mathbf{A}$  is

$$\begin{bmatrix}
 1 & 1 & -1 & 3 & -1 & 2 & 0 & 1 & -1 & 1 & -1 & 2 & -1 & -3 & -1 & -1 & 3 & 3 & 1 & 1 & 1 & 1 \\
 1 & 0 & 1 & 0 & 1 & 1 & 0 & 0 & 1 & 0 & 1 & 0 & 1 & 1 & 1 & 1 & 0 & 0 & 0 & 0 & 0 & 0 \\
 -2 & -1 & -2 & 0 & -2 & -2 & -1 & 0 & -1 & 0 & -2 & 0 & -2 & 0 & -2 & -2 & 0 & 0 & -2 & 0 & 0 & 0 \\
 a_1 & a_2 & a_3 & a_4 & a_5 & a_6 & a_7 & a_8 & b_1 & b_2 & b_3 & b_4 & b_5 & b_6 & b_7 & b_8 & b_9 & b_{10} & b_{11} & c_1 & c_2 & a
 \end{bmatrix} \cdot$$

unknowns

We can solve the general form of Eq. (7) and obtain a system of the fundamental solutions in the analysis procedure. It is clear that the rank of  $\mathbf{A}$  is 3. That is, Eq. (7) includes 3 independent and 19 dependent variables, which can form 19 linearly independent fundamental solutions. Different orders of column vectors in dimensional matrix  $\mathbf{A}$  might lead to different structures of solution, but the solution space is always the same.

Generally, we tend to have a specific purpose in dimensional analysis for deriving some useful dimensionless qualities. For example, if we want to emphasize the importance of dynamic viscosity ( $\eta$ ), pore water pressure ( $p_p$ ) and permeability ( $k$ ), these three parameters will be chosen as independent variables, while others are the dependent variables. Accordingly, the dimensional matrix is rewritten as  $\mathbf{A}_1$

$$\begin{bmatrix}
 -1 & -1 & 2 & -1 & 1 & -1 & -3 & -1 & 3 & 3 & 1 & 1 & 1 & -1 & 3 & -1 & 2 & 0 & 1 & 1 & 1 & 1 \\
 1 & 1 & 0 & 1 & 0 & 1 & 1 & 1 & 0 & 0 & 0 & 1 & 0 & 1 & 0 & 1 & 1 & 0 & 0 & 0 & 0 & 0 \\
 -1 & -2 & 0 & -2 & 0 & -2 & 0 & -2 & 0 & 0 & -2 & -2 & -1 & -2 & 0 & -2 & -2 & -1 & 0 & 0 & 0 & 0 \\
 b_1 & b_3 & b_4 & b_7 & b_2 & b_5 & b_6 & b_8 & b_9 & b_{10} & b_{11} & a_1 & a_2 & a_3 & a_4 & a_5 & a_6 & a_7 & a_8 & c_1 & c_2 & a
 \end{bmatrix} \cdot$$

unknowns

Let  $y_1=(b_1, b_3, b_4, b_7, b_2, b_5, b_6, b_8, b_9, b_{10}, b_{11}, a_1, a_2, a_3, a_4, a_5, a_6, a_7, a_8, c_1, c_2, a)^T$ , then solve  $\mathbf{A}_1 y_1=0$ . If a column vector  $\xi_j$  ( $j=1,2,\dots,19$ ) is a fundamental solution, then 19 fundamental solutions form a matrix  $\xi$ , which can be divided into two parts: a 19-order identity matrix  $\mathbf{I}$  and a  $3 \times 19$  affecting factors matrix  $\mathbf{B}$ ,  $\xi=[\mathbf{B} \mathbf{I}]^T$ . The matrix  $\mathbf{B}$  reads:

$$\begin{bmatrix} 0 & 0 & 0 & -2 & 0 & 0 & 0 & 2 & 0 & 1 & 0 & 0 & 0 & 0 & 1 & 0 & 0 & 0 & 0 \\ -1 & 0 & -1 & 1 & -1 & 0 & 0 & -2 & -1 & -1 & -1 & 0 & -1 & -1 & -1 & 0 & 0 & 0 & 0 \\ 0 & -\frac{1}{2} & 0 & 1 & 0 & -\frac{3}{2} & -\frac{3}{2} & -\frac{1}{2} & -1 & -\frac{1}{2} & 0 & -\frac{3}{2} & 0 & -\frac{3}{2} & 0 & -\frac{1}{2} & -\frac{1}{2} & -\frac{1}{2} & -\frac{1}{2} \end{bmatrix}.$$

Let  $\xi_{ij}$  ( $i=1,2, \dots, 22$ ) be an element of  $\xi_j$ . A power law behavior between variables yields the following equation

$$\pi_j = \prod_{i=1}^{22} (Var_i)^{\xi_{ij}} \tag{8}$$

where  $Var=(Var_j)=(F, v, p_j, Q_j, p_b, N_c, w_c, D_c, \eta, D, p_p, k, p_f, \rho, E_e, \sigma, V_g, V_p, g, H, R, S_{max})^T$  is a column vector including 21 influence factors and the maximum settlement  $S_{max}$ . For example, according to the fourth column, the function expression can be written as

$$\pi_4 = \rho k p_p \eta^{-2} \tag{9}$$

### 5. DIMENSIONLESS QUANTITIES AND EXPERIMENTAL VERIFICATION

The dimensionless quantities are extremely helpful for a deep insight into a complex problem arising mechanical engineering. Zhao suggested a dimensionless number for a beam’s dynamic plastic response [50], Lesur and Longaretti [51] showed that the dimensionless numbers can identify fast and reliably the magnet-rotational instability with ease, while Zinola [52] adopted the dimensionless theory to study an extremely complex reaction process. Scientists word to decipher how a complex problem is resolved using the dimensionless analysis, without introducing some reliable dimensionless quantities. The success presented in [50,51] is questionable.

#### 5.1. Dimensionless Quantities

Now we turn back to our analysis and introduce three important dimensionless numbers, a soil dimensionless number ( $S$ ), a dimensionless number for the shield tunneling machine ( $TM$ ), and a geometrical dimensionless number for the tunnel ( $G$ ).

1) The soil dimensionless number is defined as

$$S = \frac{p_p^{a+b+c-d} \mathbf{k}^d}{E_e^a p_f^b \sigma^c v^d D^d (1-r)^e} \tag{10}$$

2) The dimensionless number for the shield tunneling machine

$$TM = \frac{p_b^q N_c^s W_c^t D_c^u}{F^{(6s-6p+2u-t)/4} Q_j^p p_j^{(6p+4q-2s+3t+2u)/4} v^{(4u+t)/2}} \tag{11}$$

3) The geometrical dimensionless number

$$G = \left( \frac{R}{H} \right)^m \quad (12)$$

where  $a, b, c, d, e, p, q, s, t, u$  and  $m$  are indexes which can be determined experimentally, and they satisfy  $a+b+c-d>0$ ,  $6s-6p+2u-t>0$ ,  $6p+4q-2s+3t+2u>0$ ,  $4u+t>0$ ;  $\kappa$  is the soil permeability coefficient, and  $r$  is the porosity

$$\kappa = k\rho g/\eta, \quad r = \frac{V_p}{V_g} \quad (13)$$

The soil dimensionless number is used to determine the type of surface settling pattern as safe or unsafe during the tunneling process. According to the definition given in Eq. (10), a higher permeability coefficient ( $\kappa$ ) of strata and a larger porosity ( $r$ ) will lead to a larger value of the soil dimensionless number, implying a larger surface settlement. When the soil dimensionless number reaches a threshold value, an unsafe surface settling process occurs. The indexes involved in Eq. (10) might be relative fractal dimensions of the porous soil. For example, the index of the porosity can be calculated by the following He-Liu's fractal dimension formulation [34]:

$$e = 3r \quad (14)$$

Here, when the porosity  $r=1$ , it becomes an empty volume, and when  $r=0$ , the soil can be considered as a continuum. The dimensionless quantity can be used for the drilling process by setting  $r=0$ . When the porosity tends to 1, the soil dimensionless number becomes infinitely large, and the surface settlement is totally unsafe.

The machine number of Eq. (11) shows the effects of the tunneling process on the surface settlement. A larger grouting quantity ( $Q_j$ ), or a larger grout filling pressure ( $p_j$ ) leads a smaller value of the machine number ( $TM$ ), on the other hand, a larger cutter torque ( $N_c$ ) results in a larger value of  $TM$ .

The geometrical number ( $G$ ) in Eq. (12) shows the importance of the ratio of  $R/H$ , when the cover depth ( $H$ ) tends to infinity, the geometrical number becomes zero, and the surface settlement is almost zero. When the ratio ( $R/H$ ) increases gradually, the geometrical number increases gradually, too, and an unsafe surface settlement is predicted when the ratio reaches a threshold value.

In Eq. (12), the index can be calculated by He-Liu's fractal dimension formulation [34]

$$m = 3(1-r) \quad (15)$$

The geometrical number becomes

$$G = \left( \frac{R}{H} \right)^{3-3r} \quad (16)$$

## 5.2. Experiment verification

To verify our derivation, we consider an extreme case for an elastic beam under uniform load, its maximal displacement can be easily calculated, and it follows [53]

$$w_{\max} \propto \frac{q}{E} \quad (17)$$

where  $w_{\max}$  is the maximal displacement,  $q$  is the uniform load,  $E$  is the elasticity modulus. Eq. (17) implies the case when  $a=1$ ,  $b=c=d=0$ , and  $r=0$  in Eq. (10), that is

$$S = \frac{P_p}{E_e} \tag{18}$$

This implies that the soil dimensionless number given in Eq. (10) is reasonable.

The geometrical dimensionless number also gives a better insight into the tunnel’s geometrical property. In practical applications, the tunnel is considered to be a shallow tunnel when  $H < 4R$ . If  $H > 50$ , the tunnel is considered to be a deep tunnel. The soil’s porosity was not considered. This has changed now as we can use the geometrical dimensionless number to judge accurately if a tunnel is a shallow one or a deep one. As an example, we consider the case when  $r=0.3$  and  $R=3.0$  m. Fig. 3 shows the variation law of the dimensionless number  $G$  with the ratio  $(R/H)$  for different values of the porosity. Instead of the value of  $R/H$ , the geometrical dimensionless number should be used to assess the tunnel’s geometrical property.

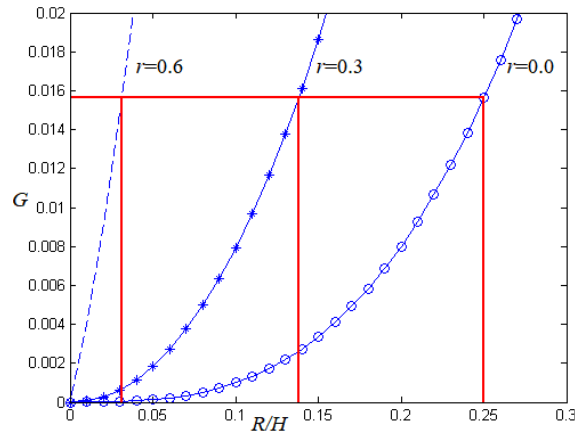


**Fig. 3** Variation law of the dimensionless number  $G$

When other parameters are set to constants, the machine dimensionless number ( $TM$ ) is inversely proportional to the penetration rate ( $v$ ), that is

$$TM \propto S_{\max} \tag{19}$$

$$S_{\max} = \alpha_1 + \beta_1 TM = \alpha_1 + \beta_1 / v^i$$

where  $i=4u+t > 0$ , according to the experimental data, we can obtain the coefficients of Eq. (19) by using the least square method.

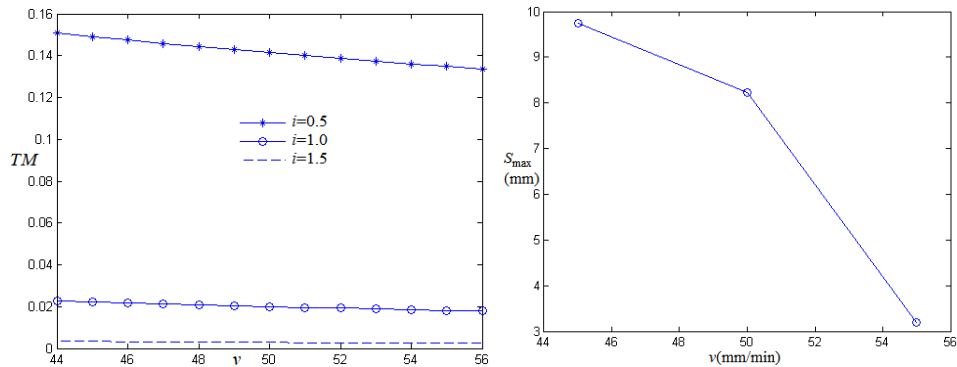
Similarly,  $TM$  is proportional to the cutter torque ( $N_c$ ), that is

$$TM \propto S_{\max} \tag{20}$$

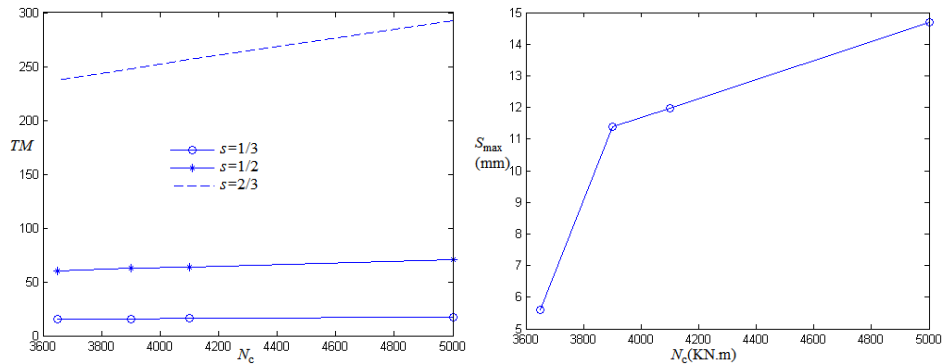
$$S_{\max} = \alpha_2 + \beta_2 TM = \alpha_2 + \beta_2 N_c^s$$

Fig. 4 shows the variation law of  $TM$  with  $v$ . It can be seen that  $TM$  decreases with the increase of  $v$ . Moreover, the variation law of  $TM$  with  $N_c$  is shown in Fig. 5. It is clear that

$TM$  increases with the increasing of  $N_c$ . According to Eq. (11), the machine number shows that a larger penetration rate leads to a smaller value of the machine number, while, on the other hand, a larger cutter torque results in a larger value of  $TM$ . In addition, it can be seen from the right parts of Figs. 4 and 5 that the dimensionless analysis results are consistent with the experimental data.



**Fig. 4** The variation law of  $TM$  (left) and  $S_{\max}$  (right) with the  $v$



**Fig. 5** The variation law of  $TM$  (left) and  $S_{\max}$  (right) with the  $N_c$

## 5. CONCLUSION

We have obtained some dimensionless numbers by dimensional analysis, which enable us to gain insight into the surface settlement with ease for various different cases, and it sheds a bright light on the tunnel's design and safety monitoring. This paper is expected to trigger much interest in the dimensionless method for various complex problems, and it can be used as a good paradigm for further applications.

This paper proposes successfully three dimensionless numbers dealing with an extremely complex problem of the surface settlement, which is crucial for the tunneling process, and the dimensionless numbers are extremely important for engineers dealing with the tunnel design and monitoring the tunneling process. Of course, the authors realize fully that, regardless of the rigor of the theoretical analysis, experimental verification is strongly required to determine the

indexes involved in the dimensionless numbers and their threshold values for the unsafe surface settlement. The dimensionless analysis provides deep insight for the analysis of the surface settlement induced by the shield tunneling. The given dimensionless numbers give reliable criteria for civil and mechanical engineers of tunneling machines as well.

**Acknowledgement:** *The authors would like to acknowledge the Deanship of Scientific Research, Taif University, for funding this work.*

#### REFERENCES

1. Chen, R.P., Zhang, P., Kang, X., Zhong, Z.Q., Liu, Y., Wu, H.N., 2019, *Prediction of maximum surface settlement caused by earth pressure balance (EPB) shield tunneling with ANN methods*, Soils and Foundations, 59(2), pp. 284-295.
2. Qi, T., Zhang, Q. H., Hu, X. D., Fan, X. J., 2010, *A practical approach for predicting surface settlements induced by shield tunneling*, Rock and Soil Mechanics, 31(4), pp. 1247-1252.
3. Koyama, Y., 2003, *Present status and technology of shield tunneling method in Japan*, Tunnelling and Underground Surface Technology, 18(2-3), pp. 145-159.
4. Wu, H.N., Shen, S.L., Liao, S.M., Yin, Z.Y., 2015, *Longitudinal structural modelling of shield tunnels considering shearing dislocation between segmental rings*, Tunnelling and Underground Surface Technology, 50(8), pp. 317-323.
5. Gao, Y.X., Liu, Y.W., Tang, P.J., Mi, C.Q., 2022, *Modification of Peck Formula to Predict Surface Settlement of Tunnel Construction in Water-Rich Sandy Cobble Strata and Its Program Implementation*, Sustainability, 14(21), 14545.
6. Lu, D., Lin, Q., Tian, Y., Du, X., Gong, Q., 2020, *Formula for predicting ground settlement induced by tunnelling based on gaussian function*, Tunnelling and Underground Space Technology, 103, 103443.
7. Yang, M., Huang, J., Sun Q., Liu K., Zeng Y.J., 2012, *Computation method for long-term surface and subsurface settlements induced by excavation of tunnels in clays*, Chinese Journal of Geotechnical Engineering, 34(2), pp. 217-221.
8. Macklin, S.R., 1999, *The prediction of volume loss due to tunneling in overconsolidated clay based on heading geometry and stability number*, Ground Engineering, 32(4), pp. 30-33.
9. Chou, W.I., Bobe,t A., 2002, *Prediction of ground deformations in shallow tunnels in clay*, Tunnelling and Underground Space Technology, 17(1), pp. 3-19.
10. Park, K.H., 2005, *Analytical solution for tunneling-induced ground movements in clays*, Tunnelling and Underground Space Technology, 20(3), pp. 249-261.
11. Topal, C., Mahmutoğlu, Y., 2021, *Assessment of surface settlement induced by tunnel excavations for the Esenler-Başakşehir (Istanbul, Turkey) Subway Line*, Environmental Earth Sciences, 80, 188.
12. Ocak, I., 2009, *Environmental effects of tunnel excavation in soft and shallow ground with EPBM: the case of Istanbul*, Environmental Earth Sciences, 59(2), pp. 347-352.
13. Ercelebi, S.G., Copur, H., Ocak, I., 2011, *Surface settlement predictions for Istanbul Metro tunnels excavated by EPB-TBM*, Environmental Earth Sciences, 62(2), pp. 357-365.
14. Chakeri, H., Ozcelik, Y., Unver, B., 2013, *Effects of important factors on surface settlement prediction for metro tunnel excavated by EPB*, Tunnelling and Underground Space Technology, 36(6), pp. 14-23.
15. Yu, W., Lei, B., Ng, M.K., Cheung, A.C., Shen, Y., Wang, S., 2022, *Tensorizing GAN with high-order pooling for Alzheimer's disease assessment*, IEEE Transactions on Neural Networks and Learning Systems, 33(9), pp. 4945-4959.
16. Wang, S., Wang, X., Shen, Y, He, B., Zhao, X., Cheung, P.W., Cheung, J.P., Luk, K.D., Hu, Y., 2020, *An ensemble-based densely-connected deep learning system for assessment of skeletal maturity*, IEEE Transactions on Systems, Man, and Cybernetics: Systems, 52(1), pp. 426-437.
17. You, S., Lei, B., Wang, S., Chui, C.K., Cheung, A.C., Liu, Y., Gan, M., Wu, G., Shen, Y., 2020, *Fine perceptive gans for brain MR image super-resolution in wavelet domain*, IEEE transactions on neural networks and learning systems, 2020, 35254996.
18. Hu, S., Lei, B., Wang, S., Wang, Y., Feng, Z., Shen, Y., 2022, *Bidirectional mapping generative adversarial networks for brain MR to PET synthesis*, IEEE Transactions on Medical Imaging, 41(1), pp. 145-157.

19. Yu, W., Lei, B., Wang, S., Liu, Y., Feng, Z., Hu, Y., Shen, Y., Ng, M.K., 2021, *Morphological feature visualization of Alzheimer's disease via multidirectional perception GAN*, IEEE Transactions on Neural Networks and Learning Systems, 2021, 35320106.
20. Suwansawat, S., Einstein, H.H., 2006, *Artificial neural networks for predicting the maximum surface settlement caused by EPB shield tunneling*, Tunneling and Underground Space Technology, 21, pp. 133-150.
21. Ocak, I., Seker, S.E., 2013, *Calculation of surface settlements caused by EPBM tunneling using artificial neural network, SVM, and Gaussian processes*, Environmental Earth Sciences, 69(5), pp. 1673-1683.
22. Ling, X., Kong, X., Tang, L., Zhao, Y., Tang, W., Zhang, Y., 2022, *Predicting earth pressure balance (EPB) shield tunneling-induced ground settlement in compound strata using random forest*, Transportation Geotechnics, 35, 100771.
23. Shen, W.J., Davis, T., Lin, D.K.J., Nachtsheim, C.J., 2014, *Dimensional analysis and its applications in statistics*, Journal of Quality Technology, 46(3), pp. 185-198.
24. Estrada-Díaz, J.A., Olvera-Trejo, D., Elias-Zúñiga, A., Martínez-Romero, O., 2021, *A mathematical dimensionless model for electrohydrodynamics*, Results in Physics, 25, 104256.
25. He, J.-H., Qian, M.-Y., Li, Y., 2022, *The maximal wrinkle angle during the bubble collapse and its application to the bubble electrospinning*, Frontiers in Materials, 8, 800567.
26. Qian, M.-Y., He, J.-H., 2022, *Collection of polymer bubble as a nanoscale membrane*, Surfaces and Interface, 28, 101665.
27. Zuo, Y.T., Liu, H.J., 2022, *Effect of temperature on the bubble-electrospinning process and its hints for 3-D printing technology*, Thermal Science, 26 (3), pp. 2499-2503.
28. He, C.H., Liu, S.H., Liu, C., Mohammad-Sedighi, H., 2022, *A novel bond stress-slip model for 3-D printed concretes*, Discrete and Continuous Dynamical Systems, 15(7), pp. 1669-1683.
29. Kong, H.Y., He, J.-H., 2012, *A novel friction law*, Thermal Science, 16(5), pp. 1529-1533.
30. Jiang, Z., Yu, C.W., Yang, J.P., Han, G.T., Xing, M.J., 2019, *Estimation of yarn strength based on critical slipping length and fiber length distribution*, Textile Research Journal, 89(2), pp.182-194.
31. Prakash, M.J., Surajkumar, G.K., Desavale, R.G., Shubham, B.P., 2020, *Distributed fault diagnosis of rotor-bearing system using dimensional analysis and experimental methods*, Measurement, 166, 108239.
32. Ma, N., 2021, *Dimensional analysis and inertial effects in transient thermal stress analysis*, Thermal Science & Engineering Progress, 22, 100787.
33. Silva, A.J.V., Pérez-Domínguez, L., Gómez, E.M., Luviano-Cruz, D., Valles-Rosales, D., 2021, *Dimensional analysis under linguistic pythagorean fuzzy set*, Symmetry, 13(3), 440.
34. He, C.H., Liu, C., 2023, *Fractal dimensions of a porous concrete and its effect on the concrete's strength*, Facta Universitatis Series: Mechanical Engineering, 21(1), pp. 137-150.
35. Jia, J., Gao, R., Wang, D., Li, J., Song, Z., Tans, J., 2022, *Settlement behaviours and control measures of twin-tube curved buildings-crossing shield tunnel*, Structural Engineering and Mechanics, 84(5), pp. 699-706.
36. Wang, Y.X., Liu, J., Guo, P.P., Zhang, W., Lin, H., Zhao, Y.L., Ou, Q., 2021, *Simplified analytical solutions for tunnel settlement induced by axially loading single pile and pile Group*, Journal of Engineering Mechanics, 147(12), pp.1024-1037.
37. Pichler, C., Lackner, R., Spira, Y., Mang, H.A., 2003, *Thermochemomechanical assessment of ground improvement by jet grouting in tunneling*, Journal of Engineering Mechanics, 129(8), pp. 951-962.
38. Tong, L.Y., Zhou, H., Shen, H., Liu, H.L., 2022, *A complex variable solution for shallow rectangular tunnel in semi-infinite plane*, Journal of Engineering Mechanics, 148(4), 4022012.
39. Li, R.J., Lei, H.Y., Ma, C.Y., Liu, Y.N., Liu, N.M., 2023, *The development of sand erosion induced by shield-tunnel joint leakage*, Engineering Failure Analysis, 148, 107068.
40. Ye, X.W., Zhang, X.L., Zhang, H.Q., Ding, Y., Chen, Y.M., 2023, *Prediction of lining upward movement during shield tunneling using machine learning algorithms and field monitoring data*, Transportation Geotechnics, 41, 101002.
41. Subel, A., Chattopadhyay, A., Guan, Y., Hassanzadeh, P., 2021, *Data-driven subgrid-scale modeling of forced Burgers turbulence using deep learning with generalization to higher Reynolds numbers via transfer learning*, Physics of Fluids, 33(3), 031702.
42. Feroudj, N., Koten, H., Boudebous, S. 2022, *Mixed Convection Heat Transfer and entropy generation in a water-filled square cavity partially heated from below: the effects of Richardson and Prandtl numbers*, Journal of Applied and Computational Mechanics, 8(1), pp. 282-297.
43. Cavallotti, C., Pelucchi, M., Georgievskii, Y., Klippenstein, S.J., 2019, *EStokTP: electronic structure to temperature- and pressure-dependent rate constants-a code for automatically predicting the thermal kinetics of reactions*, Journal of Chemical Theory and Computation, 15(2), pp.1122-1145.
44. Gajbhiye, N.L., Eswaran, 2018, *VMHD buoyant flow in a cubical enclosure at low to high Hartmann number*, International Journal of Thermal Sciences, 134, pp. 168-178.

45. He, J.-H., Elgazery, N.S., Elagamy, K., Abd Elazem, N.Y., 2023, *Efficacy of a modulated viscosity-dependent temperature/nanoparticles concentration parameter on a nonlinear radiative electromagneto-nanofluid flow along an elongated stretching sheet*, Journal of Applied and Computational Mechanics, 9(3), pp. 848-860.
46. Zhang, X., Jiao, Y., Qu, X., Huo, G., Huang, K., 2023, *Dimensional analysis of the working condition dependence on the leakage performance of a hole diaphragm labyrinth seal*, Journal of the Brazilian Society of Mechanical Sciences and Engineering, 45(4), 210.
47. Haghgoo, M., Babaei, H., Mostofi, T.M., 2023, *A non-dimensional analysis on the large plastic deformation triangular plates under impulsive loading*, Journal of the Brazilian Society of Mechanical Sciences and Engineering, 45(1), 25.
48. Zhao, Y.J., Zhang, Y.L., Zhou, F.L., 2021, *The effect of downtime on non-inertial stopping performance under special working conditions*, Journal of the Brazilian Society of Mechanical Sciences and Engineering, 42 (4), pp. 371-380.
49. Sonin, A.A., 2004, *A generalization of the  $\pi$ -theorem and dimensional analysis*, Applied Physical Science, 101(23), pp. 8525-8526.
50. Zhao, Y.P., 1998, *Suggestion of a new dimensionless number for dynamic plastic response of beams and plates*, Archive of Applied Mechanics, 68(7/8), pp. 524-538.
51. Lesur, G., Longaretti, P.Y., 2007, *Impact of dimensionless numbers on the efficiency of magnetorotational instability induced turbulent transport*, Monthly Notices of the Royal Astronomical Society, 378(4), pp. 1471-1480.
52. Zinola, C.F., 2023, *Dimensionless numbers on columnar structured electrodes in hydrogen/oxygen polymer electrolyte fuel cells*, Chemical Engineering Journal, 454(4), 140315.
53. Craig, R.R., 2011, *Mechanics of Materials* (Third edition), Wiley, 538 p.